Neural dynamics of semantic categorization in semantic variant of Primary Progressive Aphasia

Running Title:

Brain dynamics of semantic categorization in semantic variant of PPA

V. Borghesani[1], C. L. Dale[2], S. Lukic[1], L. B. N. Hinkley[2], M. Lauricella[1], W. Shwe[1], D. Mizuiri[2], S. Honma[2], Z. Miller[1], B. Miller[1], J. F. Houde[3], M.L. Gorno-Tempini[1,4] & S. S. Nagarajan[2,3]

[1] *Memory and Aging Center, Department of Neurology, University of California San Francisco*
[2] *Department of Radiology and Biomedical Imaging, University of California San Francisco*
[3] *Department of Otolaryngology, University of California San Francisco*
[4] *Department of Neurology, Dyslexia Center, University of California, San Francisco, CA*

Corresponding Author
Valentina Borghesani, PhD, valentina.borghesani@ucsf.edu
Department of Neurology,
Memory and Aging Center,
University of California San Francisco
675 Nelson Rising Lane, Mission Bay Campus,
San Francisco, CA 94158, USA

Title: 94 characters

Abstract: 200 words

Main text: 4250 words

Tables: 3

Figures: 3

Supplementary Figure: 1

Abstract

Awake humans constantly extract conceptual information from a flow of perceptual inputs. Category membership (e.g., *is it an animate or inanimate thing?*) is a critical semantic feature used to determine the appropriate response to a stimulus. Semantic representations are thought to be processed along a posterior-to-anterior gradient reflecting a shift from perceptual (e.g., *it has eight legs*) to conceptual (e.g., *venomous spiders are rare*) information. One critical region is the anterior temporal lobe (ATL): patients with semantic variant primary progressive aphasia (svPPA), a clinical syndrome associated with ATL neurodegeneration, manifest a deep loss of semantic knowledge.

Here, we test the hypothesis that svPPA patients, in the absence of an intact ATL, perform semantic tasks by over-recruiting areas implicated in perceptual processing. We acquired MEG recordings of 18 svPPA patients and 18 healthy controls during a semantic categorization task. While behavioral performance did not differ, svPPA patients showed greater activation over bilateral occipital cortices and superior temporal gyrus, and inconsistent engagement of frontal regions.

These findings indicate a pervasive reorganization of brain networks in response to ATL neurodegeneration: the loss of this critical hub leads to a dysregulated (semantic) control system, and defective semantic representations are compensated via enhanced perceptual processing.

Introduction

Approaching a greenish, twisted object during a countryside walk, you might have two very different reactions: running away or simply stepping over it. Such a seemingly easy process, i.e., telling a *snake* from a *rope*, requires the interplay of multiple cognitive processes relying on different neural substrates. First, the visual input must be analyzed, collecting information on all possibly relevant motor-perceptual features (e.g., *color, sound, movement*). Then, the extracted features must be merged into a unitary concept to allow proper identification (e.g., *it's a rope*). Finally, one can select and perform an appropriate response (e.g., *I'll walk by it*). All the neural computations supporting these processes occur within a few seconds. While the earliest perceptual processing takes place in the occipital cortex, the final stages (i.e., motor programming and execution) entail activation of frontal-parietal structures. The critical intermediate steps, involving the transformation from a visual input to a concept (and its semantic categorization as living vs. nonliving, dangerous vs. harmless), have been linked to the coordinated activity of multiple neural areas (Clarke & Tyler, 2015). Functional neuroimaging and neuropsychological research indicate that semantic knowledge is encoded within distributed networks (Huth, Nishimoto, Vu, & Gallant, 2012; Fernandino et al. 2015), with a few key cortical regions acting as critical hubs (Lambon-Ralph, Jefferies, Patterson, & Rogers, 2017). However, many open questions remain as to the nature of neural representations and computations in these different areas, and how they dynamically interact.

Prior functional neuroimaging studies suggested that populations of neurons along the ventral occipito-temporal cortex (vOT) tune to ecologically relevant categories leading to a nested representational hierarchy of visual information (Grill-Spector & Weiner, 2014), where specialized cortical regions respond preferentially to faces (Gauthier et al., 2000; Kanwisher, McDermott, & Chun, 1997), places (Epstein & Kanwisher, 1998), bodies and body parts (P. E. Downing, Wiggett, & Peelen, 2007; P. Downing & Kanwisher, 2001), or objects (Lerner, Hendler, Ben-Bashat, Harel, & Malach, 2001). Living stimuli appear to recruit lateral portions of vOT, while nonliving stimuli are highlighted in medial regions (Martin & Chao, 2001). Multiple organizing principles appear to be responsible for the representational organization of these areas, including agency and visual categorizability (Thorat, Proklova, & Peelen, 2019). Overall,

semantic representations appear to be processed in a graded fashion along a posterior-to-anterior axis: from perceptual (e.g., *snakes are elongated and legless*) to conceptual information (e.g., *a snake is a carnivorous reptile*) (Borghesani et al., 2016; Peelen & Caramazza, 2012). Notwithstanding this overall distributed view, different areas have been linked with specific computational roles: from modality-specific nodes in secondary motor and sensory areas to multimodal convergence hubs in associative cortices (Binder & Desai, 2011).

Neuropsychological findings corroborate the idea of a distributed yet specialized organization of semantic processing in the brain, supported by the interaction of a perceptual representational system arising along the occipito-temporal pathway, a semantic representational system confined to the anterior temporal lobe (ATL), and a semantic control system supported by fronto-parietal cortices (Lambon-Ralph et al., 2017). For instance, focal lesions in the occipito-temporal pathway are associated with selective impairment for living items and spared performance on nonliving ones (Blundo, Ricci, & Miller, 2006; Caramazza & Shelton, 1998; Laiacona, Capitani, & Caramazza, 2003; Pietrini et al., 1988; Sartori, Job, Miozzo, Zago, & Marchiori, 1993; Warrington & Shallice, 1984) as well as the opposite pattern (Laiacona & Capitani, 2001; Sacchett & Humphreys, 1992). Moreover, acute brain damage to prefrontal or temporoparietal cortices in the semantic control system has been linked with semantic aphasia, a clinical syndrome characterized by deficits in tasks requiring manipulations of semantic knowledge (Jefferies & Lambon Ralph, 2006).

A powerful clinical model to study the organization of the semantic system is offered by the semantic variant primary progressive aphasia (svPPA or semantic dementia, Hodges et al., 1992, Gorno-Tempini et al., 2004). This rare syndrome is associated with ATL neurodegeneration as confirmed by the observation of grey matter atrophy (Collins et al., 2016), white matter alterations (Galantucci et al., 2011), and hypometabolism (Diehl et al., 2004), as well as neuropathological findings (Hodges & Patterson, 2007). Patients with svPPA present with an array of impairments (e.g., single-word comprehension deficits, surface dyslexia, impaired object knowledge) that can be traced back to a generalized loss of semantic knowledge, often affecting all stimuli modalities and all semantic categories (Hodges & Patterson, 2007). Conversely, executive functions and perceptual abilities are relatively

115 preserved. Hence, these patients provide crucial neuropsychological evidence of the role played
116 by the ATL in the storage of semantic representations, and can be leveraged to investigate the
117 breakdown of the semantic system and the resulting compensatory mechanisms.

118 Pivotal steps forward in understanding the neurocognitive systems underlying semantic
119 (as well as any other human) behaviors are enabled by the iterative, systematic combination of
120 behavioral and neuroimaging data from both healthy controls and neurological patients (Price
121 & Friston, 2002). However, task-based imaging in patients is hampered by specific difficulties
122 (e.g., patients' compliance) and limitations (e.g., performance is not matched and error signals
123 can act as confounds) (Price, Crinion, & Friston, 2006; S. Wilson, Yen, & Eriksson, 2018). To date,
124 very few studies have attempted to deploy functional imaging in rare clinical syndromes such as
125 svPPA, thus it is still not fully clear how structural damage and functional alterations relate to
126 the observed cognitive and behavioral profile. Previous findings suggest that residual semantic
127 abilities come from the recruitment of homologous and perilesional temporal regions, as well
128 as increased functional demands on the semantic control system i.e., parietal/frontal regions
129 (Maguire, Kumaran, Hassabis, & Kopelman, 2010; Mummery et al., 1999; Pineault et al., 2019;
130 Viard et al., 2013; S. M. Wilson et al., 2009). Recently, magnetoencephalographic imaging
131 (MEG) has proven useful in detecting syndrome-specific network-level abnormalities
132 (Ranasinghe et al., 2017; Sami et al., 2018) as well as task-related functional alterations (Kielar,
133 Deschamps, Jokel, & Meltzer, 2018) in neurodegenerative patients. Critically, it has been
134 suggested that imperfect behavioral compensation can be achieved via reorganization of the
135 dynamic activity in the brain (Borghesani et al., 2020): owing to their damage to the ventral,
136 lexico-semantic reading route, svPPA patients appear to over-recruit the dorsal,
137 sublexical/phonological pathway to read not only pseudowords, but also irregular ones.

138 Here, we test the hypothesis that svPPA patients, burdened with ATL damage, thus
139 lacking access to specific conceptual representations, overemphasize perceptual information as
140 well as overtax the semantic control system to maintain accurate performance on a semantic
141 categorization task (living vs. nonliving, see Fig. 1a). Given the shallow semantic nature of the
142 task, we expect comparable performance in patients with svPPA and a group of healthy

143 controls, with the critical differences emerging in neural signatures. Specifically, we expected
144 patients to over-recruit occipital areas, supporting their greater reliance on visual processing.
145
146
147 **Results**
148
149
150 Behavioral data and cortical atrophy
151 Behavioral performance during the MEG scan neither differed between the two cohorts
152 nor between the two stimulus categories. Statistically significant differences were not observed
153 in reaction times (HC: living: 826.3±112.5, nonliving: 856.9±104.4; svPPA: living: 869.8±179.8,
154 nonliving: 911.1±194.45), or accuracy (HC: living: 84.5±5.8, nonliving: 80.4±5.4; svPPA: living:
155 80.5±6.2, nonliving: 79.1±6). Overall, these results indicate that svPPA patients can perform the
156 task as proficiently as healthy elders, an expected finding due to the relatively shallow semantic
157 processing requirements and simple stimuli used in the task (see Fig. 1b).
158 Distribution of cortical atrophy in the svPPA cohort is shown in Figure 1c. Patients
159 present atrophy in the anterior temporal lobe, involving the temporal pole, the inferior and
160 middle temporal gyrus. This pattern of neurodegeneration is consistent with their clinical
161 diagnosis and overall neuropsychological profile (see Table 1).
162

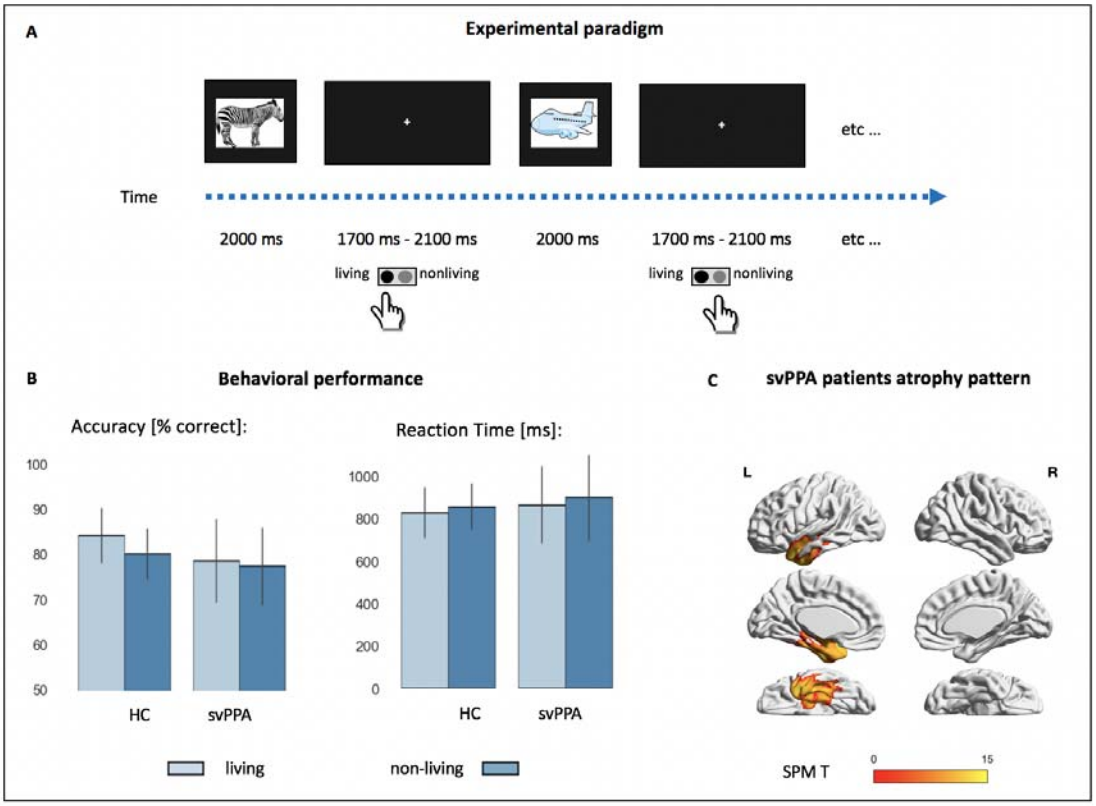

Fig. 1 Experimental paradigm, behavioral performance, and cortical atrophy. (A) Cartoon representation of the experimental setting. Colored drawings were presented for 2 seconds, with an inter-stimuli-interval jittered between 1.7 and 2.1 seconds. Subjects responded with a button press with their dominant hand. (B) Percentage accuracy and reaction times during the semantic categorization tasks in controls and svPPA patients, across the two stimuli conditions (living vs. nonliving items). (C) Voxel based morphometry (VBM)-derived atrophy pattern showing significantly reduced grey matter volumes in svPPA patients' anterior temporal lobes, views from top to bottom shown: lateral, medial, ventral (thresholded at $p<0.001$ with family wise error (FWE) correction).

Time course of neural activity during visual semantic categorization

Within-group analyses of brain activity during the semantic categorization task, relative to pre-stimulus baseline activity levels, are presented for both controls and svPPA patients in Supl. Fig. 1. In brief, following presentation of the images both cohorts showed posterior-to-anterior progression of functional activation across all five frequency bands. In the high-gamma band (63-117 Hz), we observed bilateral increases in synchronous power starting in the occipital cortex and progressively extending to temporal, parietal, and frontal regions (see Supl. Fig. 1a). In the low-gamma band (30-55 Hz), subjects show heightened synchronization over bilateral occipital cortices, evident early in the svPPA group and only later in HC. Moreover, both groups showed reductions in activity over frontal cortices starting mid-trial (see Supl. Fig. 1b). A similar

progression of alpha (8-12 Hz) and beta (12-30 Hz) band activity revealed significant reductions in synchronous activity for both groups, extending from bilateral occipital cortices to temporal and parietal lobes, and involving progressively larger areas in precentral and superior frontal gyrus. A focus of increased alpha synchrony in anterior cingulate regions, mid-trial, is evident in both groups (see Supl. Fig. 1c-d). Finally, induced theta band (3-7 Hz) activity revealed progressive increases in synchronous activity over bilateral occipital cortices, a similarly progressive pattern of increased synchronization within frontal regions at an onset window after that of occipital regions, and progressively reduced theta activity relative to baseline levels over parietal and temporal lobes (see Supl. Fig. 1e).

Taken together, these stimulus-locked task-induced changes indicate, in both cohorts and across all frequency bands, the expected pattern of visual processing followed by motor response preparation. Notwithstanding the overall similarity in spatiotemporal dynamics, specific activation differences were detected between svPPA patients and HC and are reported below.

TABLE 3. Results of MEG contrasts

	Time Window	*Local Maxima*		
t-test svPPA vs HC	*ms*	*MNI [x,y,z]*	p-value	t-value
Theta Band [3-7 Hz]				
left lingual gyrus	0 - 212	-10.0 -100.0 -10.0	0.005	3.7
left lingual gyrus	412 - 612	-8.5 -100.0 -8.1	0.005	3.1
right precentral gyrus	62 - 187	41.9 -13.6 66.2	0.005	3.4
right medial and superior frontal gyrus	187 - 412	21.8 64.0 -8.1	0.001	-3.2
Alpha Band [8-12 Hz]				
right precentral gyrus	212 -612	45.0 -15.0 40.0	0.001	3.4
left middle temporal gyrus	237- 362	-59.8 -41.6 -1.0	0.005	2.8
left anterior cingulate	462 - 612	-4.7 35.5 -9.7	0.005	3.1
left parahippocampal gyrus	512 - 612	-22.5 -49.3 -8.9	0.005	2.9
Beta Band [12-30 Hz]				
left cingulate cortex	0 - 62	-6.2 -30.3 43.3	0.005	2.9
left lingual gyrus	87 - 112	-9.3 -100.5 -13.6	0.005	2.9
right superior frontal gyrus	62 - 137	30.3 36.2 47.8	0.005	3
right medial frontal gyrus	137 - 262	7.8 56.8 11.7	0.001	3.6
left middle temporal gyrus	237 - 362	-65.0 -20.0 -5.0	0.001	-3.4
left superior frontal gyrus	562 - 612	-21.8 46.7 45.7	0.005	-3.1
Low Gamma Band [30-55 Hz]				
left lingual gyrus	62 - 612	-10.1 -98.4 -8.9	0.001	4.2
left inferior occipital gyrus	362 - 612	-34.8 -93.9 2.7	0.001	4.1
right lingual gyrus	212 - 437	18.2 -89.1 8.3	0.005	3.4
right medial frontal gyrus	212 - 412	9.3 63.0 2.2	0.001	3.7
left superior frontal gyrus	262 - 462	-3.8 62.8 14.0	0.005	3.6
High Gamma Band [63-117 Hz]				
left superior frontal gyrus	62 - 137	-36.5 26.6 48.8	0.001	3.4
left superior temporal gyrus	62 - 287	-48.2 -22.3 13.3	0.005	3
left parahippocampal gyrus	212 - 312	-15.5 -27.1 -6.5	0.001	3.3
right medial frontal gyrus	287 - 337	13.2 70.7 0.6	0.005	3.2
left superior frontal gyrus	287 - 612	-22 68.4 14	0.001	3.6
right superior frontal gyrus	462 - 612	43.9 54.7 17.2	0.001	3.9

Table 3. Local maxima in MNI coordinates. Time window, MNI coordinates, p- and t-value of the local maxima of the different MEG whole-brain contrasts performed. The spatiotemporal distribution of these clusters at 4 exemplar time points can be appreciated in Figure 2.

Neural dynamics of semantic categorization in a faulty semantic system

We investigated when, where, and at which frequency svPPA patients differ from healthy controls during semantic categorization of visual stimuli. While the overall pattern of activation across frequencies and time is similar, crucial differences between the two cohorts emerged in the between-group analyses performed in each frequency band. Table 3 summarizes the temporal windows, peaks of local maxima, and t-values of all clusters isolated by the direct comparison of the two cohorts. Figure 2 allows appreciation of the spatiotemporal distribution of these clusters at 4 exemplar time points.

In the high-gamma band, we detected significantly higher synchronization in svPPA patients, relative to controls, over left superior temporal (at both early and late time points) and right frontal (at late time points) cortices (see Fig. 2a). In the low-gamma band, we observed an extensive spatio-temporal cluster over bilateral occipital cortices with significantly higher synchronized activity in svPPA patients relative to controls. Similarly, small clusters of gamma activity, relatively more desynchronized in HC than svPPA, resulted in an increased gamma synchrony in medial frontal cortices at ~300 ms for the svPPA group (see Fig. 2b). Overall, the results at high frequencies (30-117 Hz) suggest thus higher activity in svPPA over bilateral occipital and left superior temporal cortices throughout the trial, and right frontal cortices at late time points.

Between-group contrast in beta-band revealed, in svPPA patients, more desynchronization (i.e., more beta suppression) over the left superior temporal gyrus at ~300 ms, while simultaneously displaying less desynchronization in a right middle-frontal cluster (see Fig. 2c). In the alpha-band, svPPA patients showed less desynchronization over left middle temporal gyrus at ~300 ms as well as in later clusters in the right precentral gyrus, left anterior cingulate, and left parahippocampal gyrus (see Fig. 2d). Finally, in the theta band significant differences over the left occipital cortex occurred at both early (~100 ms) and late (~500 ms) time points indicating higher synchronization in svPPA patients compared to HC, while the opposite pattern (i.e., higher activity for HC) is observed in a right frontal cluster at ~300ms (see Fig. 2e). Overall, the results at low frequencies (3-30 Hz) suggest thus higher activity in svPPA over bilateral occipital and left superior temporal cortices, while indicating less activity in left middle-temporal and right frontal regions.

Taken together, these findings suggest that svPPA patients performed the semantic categorization tasks by over-recruiting bilateral occipital cortices and left superior temporal gyrus, while showing less reliance on left middle-temporal regions and inconsistent engagement of frontal ones.

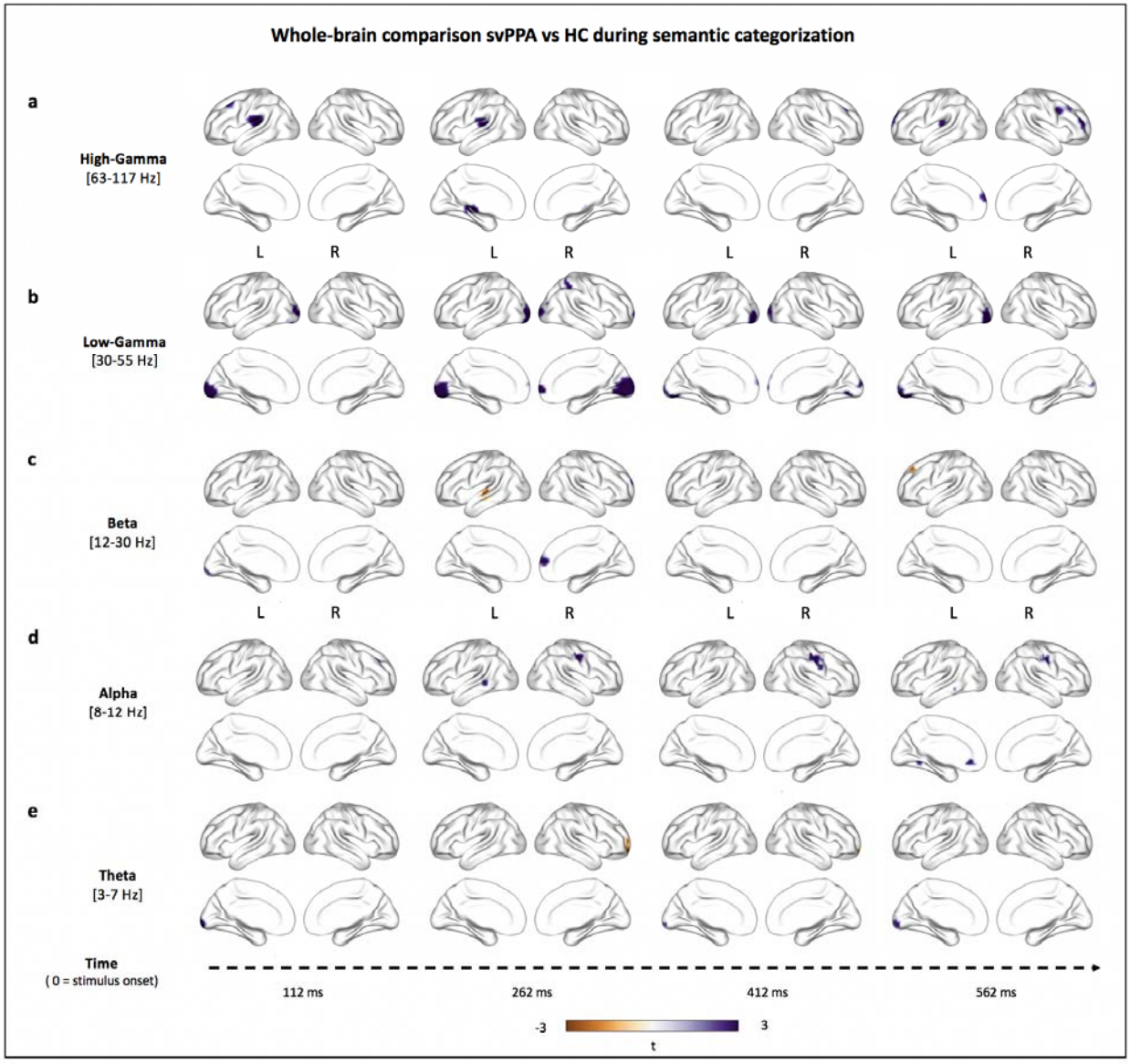

Figure 2. Stimulus-locked (0 ms = stimulus onset) between-group analyses of changes in oscillatory power. Rendering of the results in the high-gamma (a), low-gamma (b), beta (c), alpha (d) and theta (e) bands. Purple color = more synchronization in svPPA (vs. HC). Brown color = less synchronization in svPPA (vs. HC). Table 3 summarizes the temporal windows, peaks of local maxima, and t-values of all clusters isolated by the direct comparison of the two cohorts.

Occipital gamma synchronization correlates with reaction times in svPPA

As illustrated in Fig. 3, our region-of-interest (ROI) post-hoc analysis suggests a linear relation between occipital gamma synchronization and RTs in svPPA patients ($r = -0.5$, $p = 0.04$), an effect not seen in healthy controls ($r = 0.18$, $p = 0.48$). Neither of the cohorts show a

252 significant correlation between STG beta suppression and RTs (svPPA: r = 0.04, p = 0.86, HC: r =
253 -0.2, p = 0.45).

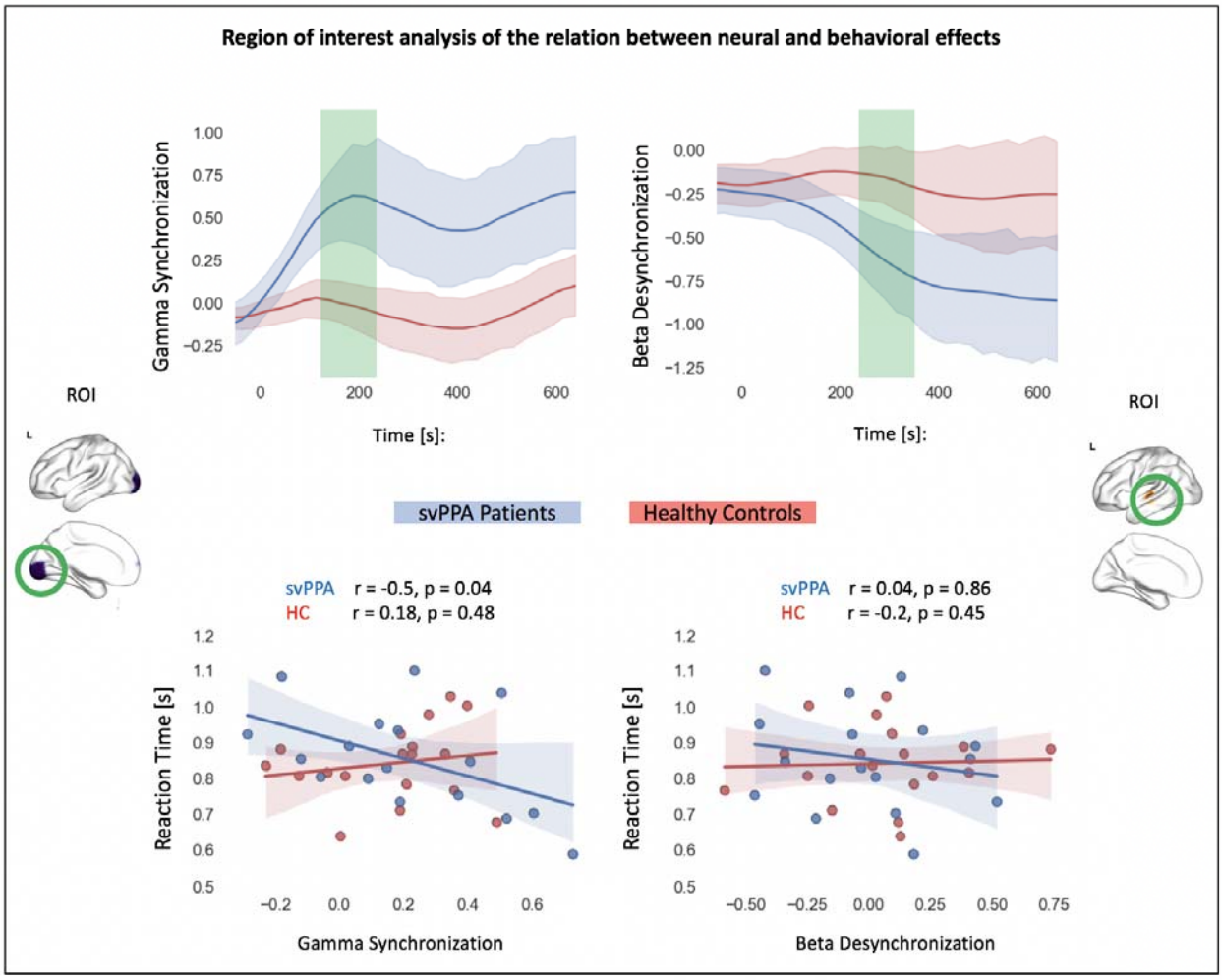

254
255 **Figure 3. Results of the region of interest post-hoc analysis correlating reaction times and beta/gamma activity.** Two ROIs
256 were centered on the main clusters resulting from the contrast svPPA patients vs. healthy controls in the gamma band (left) and
257 in the beta band (right) in the 100ms window surrounding the peak effect.
258
259 **Discussion**
260
261 This is the first study investigating the spatiotemporal dynamics of semantic
262 categorization of visual stimuli in a cohort of svPPA patients. We provide compelling evidence
263 that, burdened with ATL damage, svPPA patients recruit additional perilesional and distal
264 cortical regions to achieve normal performance on a shallow semantic task. As compared to
265 healthy age-matched controls, svPPA patients showed greater activation over bilateral occipital
266 cortices and superior temporal gyrus, indicating over-reliance on perceptual processing and

spared dorsal language networks. Conversely, they showed inconsistent engagement of frontal regions, suggesting less efficient control responses.

These findings have important implications both for current neurocognitive models of the language systems, and on the utility of MEG imaging in clinical populations. First, the detection of over-recruitment of occipital and superior-temporal regions paired with incongruous engagement of frontal ones, speaks to the distributed and dynamic organization of the semantic system, where semantic representations are supported by occipito-temporal cortices and semantic control by fronto-parietal ones. Second, the observation that normal performance can be achieved via altered neural dynamics elucidates the neurocognitive mechanisms that support compensation in neurological patients. Specifically, we contribute to the body of literature illustrating how network-driven neurodegeneration leads to the reorganization of the interplay of various cortical regions.

Faulty semantic representations: compensating conceptual loss with perceptual information

Our key finding is that svPPA patients can achieve normal performance in a shallow semantic task by over-relying on perilesional language-related regions (STG), as well as on distal visual (occipital) and executive (frontal) networks. At frequencies spanning low and high gamma bands, svPPA patients show increased activity in occipital and superior temporal cortices relative to their healthy counterparts. Gamma oscillations have been associated with local computations (Donner & Siegel, 2011), promoting unification and binding processes (Hagoort et al. 2004), including merging of multimodal semantic information (van Ackeren et al., 2014). Similarly, results at lower frequencies indicate greater neural activity in svPPA over bilateral occipital and left superior temporal cortices. Theta oscillations have been associated with operations over distributed networks, such as those required for lexico-semantic retrieval (Bastiaansen et al., 2005; Bastiaansen et al., 2008; Kielar et al., 2015) and integration of unimodal semantic features (van Ackeren et al., 2014). This data also suggests that more engagement of occipital areas (via increased gamma band activity) is related to better performance (faster RTs). In our patients, compensation for faulty semantic representations

seems thus to rely primarily on local and distributed computations in networks associated with perceptual processing.

In principle, the semantic task employed in the current study (i.e., identifying a visually presented object as either a living or nonliving) can be performed by focusing on a few key, distinctive, motor-perceptual features: *if it has eyes and teeth, it is a living being*. Further processing steps, such as would be required for an object-identification and naming (i.e., accessing the appropriate lexical label), require the integration of multiple motor-perceptual as well as conceptual features (Borghesani & Piazza, 2017): *a python is a nonvenomous snake that kills by constriction*. Combining the behavioral data collected during the recordings and outside and the scanner, it appears clear that HC can recognize (and likely inevitably mentally name) each item, while svPPA patients can only provide the categorical label. Patient data is thus critical in characterizing the division of labor between the distributed set of cortical regions involved in semantic processing. Our findings strongly suggest that ATL damage hampers operation of the semantic representation system, by shattering their conceptual components and thus forcing over-reliance on perceptual features coded in posterior cortices. This is consistent with a growing body of research. For instance, it has been shown that the ability to merge perceptual features into semantic concepts relies on the integrity of the ATL (Hoffman, Evans, & Lambon Ralph, 2014), and that ATL damage promotes reliance on perceptual similarities over conceptual ones (Lambon-Ralph, Sage, Jones, & Mayberry, 2010). Moreover, it appears that the more motor-perceptual information is associated with a given concept, the more resilient it is to damage, an advantage that is lost once the disease progresses from ATL to posterior ventral temporal regions (Hoffman, Jones, & Ralph, 2012).

Faulty semantic representations: overtaxing the semantic control network

Compared to healthy controls, svPPA patients appear to have less activation in the left middle-temporal gyrus and to inconsistently engage frontal regions, suggesting that increased demands to the semantic control systems are met by inefficient responses in prefrontal and superior frontal cortices. Comparing the two cohorts across frequency bands, it appears that an enhanced late high frequency (local neural) response occurs in svPPA, versus an earlier and

lower frequency (long range connection) response in controls. One speculation for this pattern is that in svPPA an initial inefficient response in the (semantic) cognitive control network centered on frontal areas leads to a later higher reliance on local activity for (semantic) cognitive control and decision-making processes.

Previous studies demonstrated that object recognition in visual areas is facilitated by prior knowledge (Bannert & Bartels, 2013) received via feedback projections from both frontal (Bar et al., 2006) and anterior temporal (Coutanche & Thompson-Schill, 2015) cortices. Moreover, it has been observed that higher demands for feature integration entail more recurrent activity between fusiform and ATL (Clarke, Taylor, & Tyler, 2011). Our study provides a direct contrast between subjects in which both frontal and ATL feedback inputs are preserved (HC), and those in which ATL neurodegeneration forces reliance exclusively on frontal inputs.

Interestingly, the observed temporal dynamics (with the detection of early frontal involvement) are not compatible with a strictly feedforward model of visual stimuli processing. This is in line with recent evidence that recurrent neural models are needed to explain the representational transformations supporting visual information processing (Gwilliams & King, 2019; Kietzmann, Spoerer, Sörensen, Cichy, & Hauk, 2019).

Thus, taken together, our findings corroborate the idea that the conversion from percept to concept is supported by recurrent loops over fronto-parietal and occipito-temporal regions which have been implicated in, respectively, semantic control and semantic representations (Chiou, Humphreys, Jung, & Lambon Ralph, 2018).

Clinical implications

Our findings corroborate the idea that neurodegeneration leads to the dynamic reorganization of distributed networks (Agosta et al., 2014; Guo et al., 2013), and that task-based MEG imaging can be instrumental in deepening our understanding of the resulting alterations (Borghesani et al., 2020). Ultimately, these efforts will pave the way towards treatment options, as well as better early diagnostic markers as functional changes are known to precede structural ones (Bonakdarpour et al., 2017). For instance, our results support previous neuropsychological evidence suggesting that the origin of svPPA patients' difficulties during semantic categorization tasks are linked to degraded feature knowledge rather than, as

it happens in other FTDs, to a deficit of the executive processes involved (Koenig, Smith, & Grossman, 2006).

Our results are in line with prior studies relating svPPA patients' performance on semantic tasks with respect to not only the expected hypoactivation of the left ATL and functionally connected left posterior inferior temporal lobe (Mummery et al., 1999), but also based on the patterns of hyperactivations observed in the current study. Heightened activity has been reported in periatrophic left anterior superior temporal gyrus as well as more distant left premotor cortex, and right anterior temporal lobe (Mummery et al., 1999; Pineault et al., 2019). Individual subject analyses have indicated that patients might attempt different compensatory strategies, which may vary in terms of efficiency and, crucially, would rely on the recruitment of different cortical networks (Viard et al., 2013, 2014). For instance, studies on reading have associated svPPA patients' imperfect compensation of the semantic deficit (leading to regularization errors) with over-reliance on parietal regions subserving sub-lexical processes (Wilson et al., 2009). Consistently, task-free studies of intrinsic functional networks suggest that the downregulation of damaged neurocognitive systems can be associated with the upregulation of spared ones. In svPPA patients, recent fMRI evidence shows coupling of decreased connectivity in the ventral semantic network with increased connectivity in the dorsal articulatory-phonological one (Battistella et al., 2019; Montembeault et al., 2019). Additionally, svPPA has been linked with specific spatiotemporal patterns of neuronal synchrony alterations: alpha and beta hyposynchrony in the left posterior superior temporal and adjacent parietal cortices, and delta-theta hyposynchrony in left posterior temporal/occipital cortices (Ranasinghe et al., 2017). Our findings also align with the recent observation that, during reading, svPPA patients can (imperfectly) compensate for their damage to the ventral route by over-recruiting the dorsal one (Borghesani et al., 2020). The present findings corroborate thus the idea that neurodegeneration forces the reorganization of the interplay between ventral and dorsal language networks.

Critically, the present functional neuroimaging results and their interpretation rest on the fact that the task allowed engagement of semantic processing in patients in which the semantic system is, by definition, compromised. Contrary to a more challenging task such as

naming, patients with svPPA were able to perform the semantic categorization as accurately and fast as healthy controls. Hence, probing the semantic system at the proper level of difficulty (Wilson et al., 2018), we avoided the challenging interpretation of activation maps associated with failure to perform a task (Price et al., 2006). Our findings thus call for caution when evaluating studies comparing clinical cohorts based solely on behavioral data: failing to detect a difference in performance does not necessarily correspond to similar underlying neurocognitive resources.

Limitations and future perspectives

The nature of the clinical model we adopted constrains our sample. First, even if ours is the to-date largest cohort of svPPA patients assessed with task-based functional neuroimaging, our sample size is relatively small, owing to the rareness of the disease. We thus have limited statistical power, preventing us from, for instance, further exploring brain-behavior correlations. Second, our subjects (both healthy controls and patients) are older than those reported in previous studies on semantic categorization, cautioning against direct comparisons. While it has been shown that the neural dynamics of visual processing are affected by aging, the reduced and delayed activity observed does not necessarily relate to poorer performance, but rather may be mediated by task difficulty (Bruffaerts et al., 2019). Moreover, previous evidence suggests that even if semantic processing remains intact during aging, its neurofunctional organization undergoes changes. For instance, (Lacombe, Jolicoeur, Grimault, Pineault, & Joubert, 2015) found that, during a verbal semantic categorization task, older adults exhibited behavioral performance equivalent to that of young adults, but showed less activation of the left inferior parietal cortex and more activation of bilateral temporal cortex. Finally, our task design does not allow further investigation of potential categorical effects. Future studies wishing to investigate representations of living and nonliving items separately will require more trials and stimuli carefully controlled for psycholinguistic variables such as prototypicality and familiarity. Contrary to patients with damage to the ventral occipito-temporal cortex due to stroke or herpes simplex encephalitis, svPPA patients usually do not present categorical dissociations (Moss, Rodd, Stamatakis, Bright, & Tyler, 2005). However, deeper investigations of time-resolved neural activity in svPPA could shed light onto the debate

on the nature of ATL representations: category-specific deficits might arise from lacunar (rather than generalized) impairment of graded representations (Lambon Ralph, Lowe, & Rogers, 2007).

Conclusions

Combining task-based MEG imaging and a neuropsychological model, we provide novel evidence that faulty semantic representations following ATL damage can be partially circumvented by additional processing in relatively spared occipital and dorsal stream regions. Our results thus inform current neurocognitive models of the semantics system by corroborating the idea that it relies on the dynamic interplay of distributed functional neural networks. Moreover, we highlight how MEG imaging can be leveraged in clinical populations to study compensation mechanisms such as the recruitment of perilesional and distal cortical regions.

Materials and methods

Subjects

Eighteen svPPA patients (13 female, 66.9 ± 6.9 years old) and 18 healthy age-matched controls (11 female, 71.3 ± 6.1 years old) were recruited through the University of California San Francisco (UCSF) Memory and Aging Center (MAC). All subjects were native speakers, and had no contraindications to MEG. Patients met currently published criteria as determined by a team of clinicians based on a detailed medical history, comprehensive neurological and standardized neuropsychological and language evaluations (Gorno-Tempini et al., 2011). Besides being diagnosed with svPPA, patients were required to score at least 15 out of 30 on the Mini-Mental Status Exam (MMSE; Folstein, Folstein, & McHugh, 1975) and be otherwise sufficiently functional to be scanned. Healthy controls were recruited from the University of California San Francisco Memory and Aging Center (UCSF MAC) healthy aging cohort, a collection of subjects with normal cognitive and neurological exam and MRI scans without clinically evident strokes. Inclusion criteria required the absence of any psychiatric symptoms or cognitive deficits (i.e., Clinical Dementia Rating - CDR = 0, and MMSE ≥28/30). Demographic

443 information and neuropsychological data are shown in Table 1. The study was approved by the
444 UCSF Committee on Human Research and all subjects provided written informed consent.
445

Table 1 Demographics and neuropsychological profiles. Healthy controls and semantic variant of Primary Progressive Aphasia (svPPA) patients, native English speakers, were matched for age, gender and education. Scores shown are mean (standard deviation). * indicate values significantly different from controls (P<0.05). MMSE = Mini-Mental State Exam; CDR = Clinical Dementia Rating; PPVT = Picture Vocabulary Test; WAB = Western Aphasia Battery; VOSP = Visual Object and Space Perception Battery.

TABLE 1. Demographics and neuropsychological profiles

	Controls	*svPPA*
Demographic		
N	18	18
Age, mean (SD)	70.7 ± 6.5	67.1 ± 6.2
Education, mean (SD)	17.5 ± 1.8	17.9 ± 3.2
Gender, *n* female	12	9
Handedness, *n* right	15	15
MMSE (max 30)	29.0 ± 1.6	24.5 ± 3.8*
CDR score	0.03 ± 0.1	0.7 ± 0.4*
CDR Box score	0.3 ± 1.2	4.0 ± 2.6*
Language Production		
Boston (object) naming test (15)	14.7 ± 0.6	5.4 ± 3.7*
Phonemic (D-letter) fluency	15.7 ± 5.8	9.1 ± 4.3*
Semantic (animal) fluency	23.4 ± 3.9	9.3 ± 4.1*
Language Comprehension		
PPVT (max 16)	---	9.4 ± 3.2
WAB Auditory Word Recognition (60)	---	56.5 ± 4.2
WAB Sequential Command (100)	---	70.7 ± 14.3
Digit Span forwards	7.1 ± 1.1	6.4 ± 1.2
Reading		
Arizona Reading Total (max 36)	35.6 ± 0.5	30.5 ± 3.7*
Regular High Frequency Words (9)	9 ± 0.0	8.8 ± 0.4
Regular Low Frequency Words (9)	8.9 ± 0.2	8.3 ± 1.2
Irregular High Frequency Words (9)	8.9 ± 0.3	7.7 ± 0.6
Irregular Low Frequency Words (9)	8.8 ± 0.4	5.7 ± 2.3
PseudoWords (18)	15.8 ± 2.7	15.2 ± 2.2
Spelling		
Arizona Spelling Total (max 20)	18.1 ± 1.6	13.1 ± 4.0*
Regular High Frequency Words (5)	5 ± 0.0	4.4 ± 0.9
Regular Low Frequency Words (5)	4.5 ± 0.6	4.1 ± 0.8
Irregular High Frequency Words (5)	4.1 ± 0.9	2.1 ± 1.6
Irregular Low Frequency Words (5)	4.5 ± 0.5	2.6 ± 1.6
PseudoWords (10)	8.8 ± 1.3	8.1 ± 2.6
Famous Faces- Spontaneous Naming (max 16)	12.4 ± 3.4	2.9 ± 2.4*
Famous Faces- Face Recognition (max 20)	18.4 ± 2.0	12.8 ± 6.5*
Famous Faces Short Triplets, Pictures (max 10)	8.9 ± 1.0	6.6 ± 2.4
Famous Faces Short Triplets, Words (max 10)	9.7 ± 0.6	7.0 ± 2.0
Working Memory/Executive functions		
Digit Span backwards	5.4 ± 1.1	4.5 ± 1.6*
Modified Trials (total time)	25.3 ± 13.6	41.9 ± 23.1*
Modified Trials (# of correct lines)	13.2 ± 3.2	13.2 ± 3.3
Design Fluency (# of correct designs)	11.7 ± 3.0	7.1 ± 3.4*
Visuospatial function		
Benson figure copy (17)	15.7 ± 0.7	15.3 ± 1.0
VOSP Number Location (30)	9.3 ± 0.9	9.0 ± 1.5
Visual memory		
Benson figure recall (17)	12.1 ± 2.4	7.1 ± 4.9*

Stimuli and Experimental Design

All subjects performed a semantic judgment task on visually presented stimuli (Figure 1a). Stimuli consisted of 70 colored drawings: 36 belonging to the semantic category of living items (e.g., animals, plants), and 34 belonging to the semantic category of nonliving items (e.g., tools, furniture).

To validate the set of stimuli, a behavioral study was conducted on a separate group of 54 age-matched healthy subjects (31 women; 47 right-handed; age = 74.21 years ± 8.63; education = 15 years ± 2.02). First, subjects had to report the most common name for each drawing (i.e., "*Identify the item in the image: what is the first name that comes to mind?*"). They were given the possibility of providing a second term if needed (i.e., "*If appropriate, write the second name that came to mind.*"). They were then asked to rate how familiar they are with the item on a 7-point scale from "*not at all familiar*" to "*very familiar*". Finally, they were asked whether the item belongs to the category of living or nonliving items, and to rate how prototypical for that category the item is (i.e., "*How good is this picture as example of an item of that category?")* on a 7-point scale from "*bad example*" to "*good example*". Data were collected with Qualtrics software (Qualtrics, Provo, UT, USA. https://www.qualtrics.com) and subjects recruited from the broad pool of subjects enrolled in the above described UCSF MAC healthy aging cohort. For each stimulus, we calculated the percentage of agreement with our pre-set categorization, average familiarity, average prototypicality, and then compared the living and nonliving categories. For living items, the average percentage of agreement with the assigned category was 96.86% ± 4.07, the lowest score was 75.93% for the item "*dinosaur*". For non-living items, the average percentage of agreement was 99.18% ± 1.20, the lowest score was 96.30% for the items "*pizza*" and "*hamburger*". A two-tailed t-test revealed that the difference between the two categories was significant (p=0.002): the rate of agreement was higher for nonliving items than for living ones. The average prototypicality of living items was 6.24 ± 0.52 (range 6.74 to 4), while for nonliving items 6.47 ± 0.32 (range 6.85 to 5.19) for nonliving items. Again, a two-tails t-test revealed a significant difference between the two categories (p=0.032): nonliving items were judged more prototypical of their category than living ones. As for familiarity, the average for living items was 6.15 ± 0.32 (range 6.8 to 4.81),

while for nonliving items was 6.67 ± 0.21 (range 6.91 to 6.02). Even in this case the difference between the two categories was significant (two-tails t-test, $p<0.001$): nonliving items were judged more familiar.

Images of the two categories were also compared in terms of visual complexity (calculated as Shannon entropy via the python package Scikit-Image, https://scikit-image.org/). No significant difference between living (3.04 ± 0.84) and nonliving (3.13 ± 0.96) items emerged. Finally, we compared stimuli in terms of the length (number of letter), imaginability, concreteness, and familiarity of their most common lexical label as extracted from the Medical Research Council (MRC, http://websites.psychology.uwa.edu.au/school/MRCDatabase/uwa_mrc.htm) Psycholinguistic Database, and word frequency was extracted from the Corpus of Contemporary American English (COCA, https://www.wordfrequency.info/). Consistent with our online questionnaire, the only statistically significant differences between the two categories were imaginability (living: 613.19± 19.62, nonliving: 596.43.15 ± 28.08, $p=0.03$) and familiarity (living: 498.26 ± 69.32, nonliving: 547.96 ± 45.82, $p<0.001$). All the psycholinguistic variables characterizing the stimuli are shown in Table 2.

Visual stimuli were projected into the magnetically shielded MEG scanner room via a system of mirrors mounted within the scanner room for this purpose, with the final mirror positioned roughly 24" from the subject's face. Subjects were instructed to classify the pictures as living or nonliving by pressing one of two response buttons with their dominant hand. Stimuli were displayed for 2 seconds, with an inter-stimulus interval jittered between 1.7 and 2.1 seconds. A total of 170 trials were presented: each individual stimulus was repeated 2.5 times in a random order. E-Prime (https://pstnet.com/products/e-prime/) was used to present the stimuli; events from ePrime and the response pad were automatically routed into the imaging acquisition software and integrated with magnetoencephalographic traces in real time.

TABLE 2. Stimuli

	Living Items	*Nonliving Items*	
N	36	34	
Examples	*fish, flower*	*scissors, train*	
Frequency (log)	3.69 (0.54)	3.96 (0.65)	
Length (# of letters)	5.29 (1.58)	5.61 (1.84)	
Immaginability	613.19 (19.62)	596.43 (28.08)	*
Familiarity (norm)	498.26 (69.32)	547.96 (45.82)	*
Familiarity (quest)	6.15 (0.32)	6.67 (0.21)	*
Concreteness	608.27 (16.26)	599.10 (25.94)	
Cat. Agreement	96.86 (4.07)	99.18 (1.20)	*
Cat. Prototypicality	6.24 (0.52)	6.47 (0.32)	*
Visual Complexity	3.04 (0.84)	3.13 (0.96)	

Table 2. Psycholinguistic characteristics of the stimuli. Stimuli consisted of 70 colored drawings illustrating living items (n=36) or nonliving items (34). Length, Imaginability, Concreteness, and Familiarity (norm) were extracted from the Medical Research Council (MRC) Psycholinguistic Database searching for the most common label for each item. Similarly, Frequency was extracted from the Corpus of Contemporary American English (COCA). Category Agreement, Category prototypicality, and Familiarity (quest.) were assessed with a behavioral study on separate age-matched healthy controls. As a proxy for Visual Complexity, we used Shannon entropy as computed with Scikit-Image. Values shown are mean (standard deviation). * indicate values significantly different between the two categories (two-tailed t-test, $p<0.05$).

Behavioral analyses

Subject performance, i.e. reaction times (RTs) and accuracy, was analyzed using an analysis of variance (ANOVA) based on the two stimuli categories (living vs. nonliving) and two cohorts (controls vs. svPPA patients) using the Python statistical library (statsmodels - www.statsmodels.org). Data from one outlier in the svPPA cohort were excluded from the behavioral analyses (average reaction times were 1.35 s versus 0.8 ms in the whole cohort).

MRI protocol and analyses

Structural T1-weighted images were acquired on a 3T Siemens system (Siemens, Erlagen, Germany) installed at the UCSF Neuroscience Imaging Center, equipped with a standard quadrature head coil with sequences previously described (Mandelli et al., 2014). MRI scans were acquired within 1 year of the MEG data acquisition.

To identify regions of atrophy, svPPA patients were compared to a separate set of 25 healthy controls collected using the same protocol (14 females, mean age 66.2 ± 8.5) via voxel-based morphometry (VBM). Image processing and statistical analyses were performed using the VBM8 Toolbox implemented in Statistical Parametric Mapping (SPM8, Wellcome Trust Center for Neuroimaging, London, UK, http://www.fil.ion.ucl.ac.uk/spm) running under Matlab

R2013a (MathWorks). The images were segmented into grey matter, white matter, and CSF, bias corrected, and then registered to the Montreal Neurological Institute (MNI). Grey matter value in each voxel was multiplied by the Jacobian determinant derived from the spatial normalization to preserve the total amount of grey matter from the original images. Finally, to ensure the data are normally distributed and compensate for inexact spatial normalization, the modulated grey matter images were smoothed with a full-width at half-maximum (FWHM) Gaussian kernel filter of 8x8x8 mm. A general linear model (GLM) was then fit at each voxel, with one variable of interest (group), and three confounds of no interest: gender, age, education, and total intracranial volume (calculated by summing across the grey matter, white matter and CSF images). The resulting statistical parametric map (SPM) was thresholded at $p<0.001$, with family wise error (FWE) correction, and a cluster extent threshold of 100 voxels. This SPM was additionally used as a binarized image of atrophy to act as an exclusive mask for the MEG source reconstruction results visualization (see below).

MEG protocol and analyses

Neuromagnetic recordings were conducted using a whole-head 275 axial gradiometer MEG system (Omega 2000, CTF, Coquitlam, BC, Canada) at a sampling rate of 1200 Hz, under a bandpass filter of 0.001 to 300 Hz, while subjects performed the task. Subjects were lying supine, with their head supported near the center of the sensor array. Head position was recorded before and after each scan using three fiducial coils (nasion, left/right preauricular) placed on the subject. All subjects included in the current study reported movement under 5 mm during the experimental run. Twenty-nine reference sensors were used to correct distant magnetic field disturbance by calculating a synthetic 3rd order gradiometer (Weinburg et al., 1984; Vrba and Robinson, 2001), which was applied to signal post-acquisition. Datasets were epoched with respect to stimulus presentation onset (stimulus-locked trials from -0.5 to 1.0 sec) and artifacts rejected using a semi-automated process outlined as follows: noisy channels were identified as having more than 20 trials exceeding 1.5pT amplitude under a temporary bandpass filter of 3 to 50 Hz, with no more than 5 channels in the sensor array removed. Epochs were then flagged and removed for any remaining artifacts exceeding the 1.5pT threshold. Mean number of trials included in analyses for the two groups did not significantly

differ (svPPA mean = 155 trials [std dev = 20, range 121-170], control mean = 162 [std dev = 16, range 103-172], 2-tailed t[34]=1.059, p=.297).

Alignment of structural and functional images was performed using 3 prominent anatomical points (nasion and preauricular points), marked in the individuals' MR images and localized in the MEG sensor array using the 3 fiducial coils attached to these points during the MEG scan. A 3D grid of voxels with 5mm spatial resolution covering the entire brain was created for each subject and recording, based on a multisphere head model of the coregistered structural 3D T1-weighted MR scan. Reconstruction of whole brain oscillatory activity within these voxels was performed via the Neurodynamic Utility Toolbox for MEG (NUTMEG; http://nutmeg.berkeley.edu), which implements a time–frequency optimized adaptive spatial filtering technique to estimate the spatiotemporal estimate of neural sources. The tomographic volume of source locations was computed using a 5 mm lead field that weights each cortical location relative to the signal of the MEG sensors (Dalal et al., 2008).

We sought to investigate both evoked and induced changes in brain activity, i.e. to study modulations of ongoing oscillatory processes that are not necessarily phased-locked (Makeig et al., 2004). Moreover, we wished to explore both high and low frequency ranges as they bear different functional interpretations, in particular their association with different spatial scales: high-frequency and low-frequency oscillations are associated with local and distributed computations, respectively (Donner & Siegel, 2011). Thus, we examined task-related modulations of ongoing oscillatory processes in 5 frequency bands: theta (3-7 Hz), alpha (8-12 Hz), beta (12-30 Hz), low-gamma (30-55 Hz) and high-gamma (63-117 Hz) (FIR filter having widths of 300 ms for theta/alpha, 200 ms for beta, 150 ms for low-gamma, and 100 ms for high-gamma; sliding over 25 ms time windows). Source power for each voxel location in a specific time window and frequency band was derived through a noise-corrected pseudo-F statistic expressed in logarithmic units (decibels; dB), describing signal magnitude during an "active" experimental time window relative to an equivalently-sized, static pre-stimulus baseline "control" window (Robinson & Vrba, 1999). Single subject beamformer reconstructions were spatially normalized by applying each subject's T1-weighted transformation matrix to their statistical map.

Group analyses were performed on normalized reconstructions using statistical nonparametric mapping (SnPM, Singh et al, 2003), both within-group and between-groups. Three-dimensional average and variance maps across subjects were calculated at each time point and smoothed with a 20 x 20 x 20mm^3 Gaussian kernel (Dalal et al., 2008). From this map, pseudo-t statistics evaluated the magnitude of the contrast obtained at each voxel and time. Voxel labels were permuted to create a T-distribution map for within- and between- group contrasts (2^N permutations, where N = number of subjects, up to 10,000 permutations). Each voxel's t-value was evaluated using 2^N degrees of freedom to determine the corresponding p-value associated with each voxel's pseudo-F value (Singh, Barnes, & Hillebrand, 2003). For uncorrected p-values attaining a threshold of $p < .005$, a cluster correction was applied, whereby cortical significance maps were thresholded, voxel-wise, under an additional requirement to have 26 adjacent significant voxels. To remove potential artifacts due to neurodegeneration or eye movement (lacking electrooculograms), we masked statistical maps using patients' ATL atrophy maps (see section MRI protocol and analyses), as well as a ventromedial frontal mask [MNI coordinates: -70 70; 5 75; -60 -10]. We utilized these to examine the pattern of activation during semantic categorization separately for controls and svPPA patients (SnPM one-sample t-test against baseline) and directly compare svPPA patients and controls to highlight spatiotemporal clusters of differential activity between the two cohorts (SnPM two-sample t-test).

Finally, we conducted a region-of-interest (ROI) post-hoc analysis aimed at investigating the relation between subjects' behavioral performance and neural activity. Two ROIs were centered on the main clusters resulting from the contrast svPPA patients vs. healthy controls in the gamma band (occipital lobe, coordinates: [-15 -5], [-105 -95], [-15 -5]) and in the beta band (temporal lobe, coordinates: [-70 -60], [-25 -15], [-10 0]). Single subjects' values were extracted in both ROIs in the 100ms window surrounding the peak effect (gamma-band peak: 112-212 ms, beta-band peak: 237-337 ms) and correlated with the reaction times.

Data Availability

The clinical and neuroimaging data used in the current paper are available from the corresponding author, upon reasonable request. The sensitive nature of patients' data and our current ethics protocol do not permit open data sharing at this stage.

Acknowledgements

The authors thank the patients and their families for the time and effort they dedicated to this research.

Funding

This work was funded by the following National Institutes of Health grants (R01NS050915, K24DC015544, R01NS100440, R01DC013979, R01DC176960, R01DC017091, R01EB022717, R01AG062196). Additional funds include the Larry Hillblom Foundation, the Global Brain Health Institute and UCOP grant MRP-17-454755. These supporting sources were not involved in the study design, collection, analysis or interpretation of data, nor were they involved in writing the paper or the decision to submit this report for publication.

Competing interests

The authors declare no competing interests.

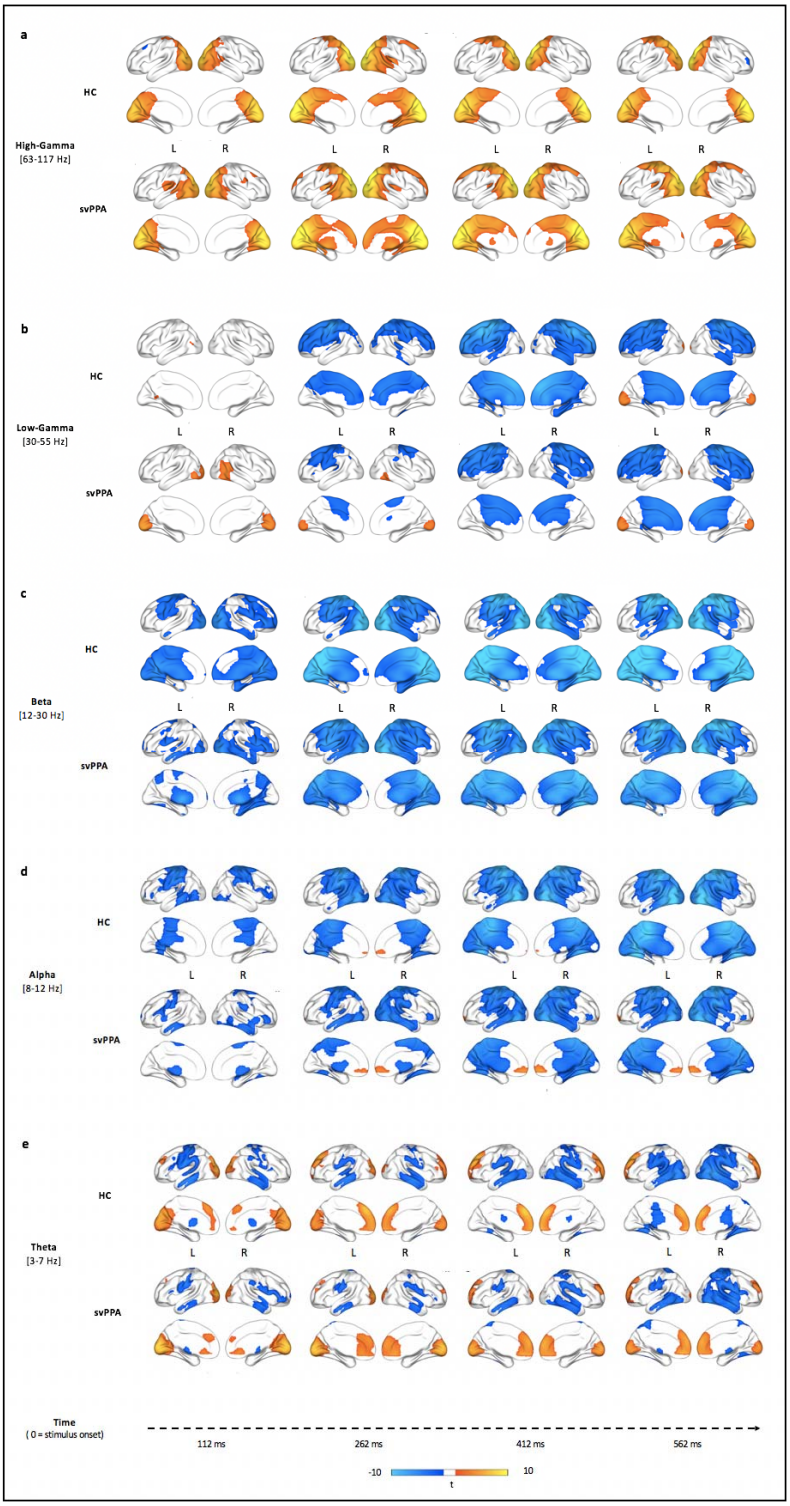

Supl. Fig. 1. Stimulus-locked (0 ms = stimulus onset) within-group analyses of task-related changes in oscillatory power. a) Rendering of the results in the high-gamma band for both controls (HC, upper row) and patients (svPPA, lower row). Cold color = more desynchronization (vs. baseline). Warm color = more synchronization (vs. baseline). c-d) Same as in (a) but for the low-gamma, beta, alpha, and theta band respectively. For details, please see text.

Bibliography

Agosta, F., Galantucci, S., Valsasina, P., Canu, E., Meani, A., Marcone, A., … Filippi, M. (2014). Disrupted brain connectome in semantic variant of primary progressive aphasia. Neurobiology of Aging, 35(11), 2646–2655. https://doi.org/10.1016/j.neurobiolaging.2014.05.017

Bannert, M. M., & Bartels, A. (2013). Decoding the yellow of a gray banana. *Current Biology*, *23*(22), 2268–2272. https://doi.org/10.1016/j.cub.2013.09.016

Bar, M., Kassam, K. S., Ghuman, A. S., Boshyan, J., Schmidt, A. M., Dale, A. M., … Halgren, E. (2006). Top-down facilitation of visual recognition. *Proceedings of the National Academy of Sciences of the United States of America*, *103*(2), 449–454. https://doi.org/10.1073/pnas.0507062103

Bastiaansen MC, Oostenveld R, Jensen O, Hagoort P (2008) I see what you mean: theta power increases are involved in the retrieval of lexical semantic information. Brain Lang 106:15-28.

Bastiaansen MC, Van Der Linden M, Ter Keurs M, Dijkstra T, Hagoort P (2005) Theta responses are involved in lexical—Semantic retrieval during language processing. Journal of cognitive neuroscience 17:530-541

Battistella, G., Henry, M., Gesierich, B., Wilson, S. M., Borghesani, V., Shwe, W., … Gorno-Tempini, M. L. (2019). Differential intrinsic functional connectivity changes in semantic variant primary progressive aphasia. *NeuroImage: Clinical*, *22*(March), 101797. https://doi.org/10.1016/j.nicl.2019.101797

Benjamini, Y., & Hochberg, Y. (2000). On the Adaptive Control of the False Discovery Rate in Multiple Testing With Independent Statistics. *Journal of Educational and Behavioral Statistics*, *25*(1), 60–83. https://doi.org/10.3102/10769986025001060

Binder, J. R., & Desai, R. H. (2011). The neurobiology of semantic memory. *Trends in Cognitive Sciences*, *15*(11), 527–536. https://doi.org/10.1016/j.tics.2011.10.001

Blundo, C., Ricci, M., & Miller, L. (2006). Category-specific knowledge deficit for animals in a patient with herpes simplex encephalitis. *Cognitive Neuropsychology*, *23*(8), 1248–1268. https://doi.org/10.1080/02643290600896449

Bonakdarpour, B., Rogalski, E. J., Wang, A., Sridhar, J., Mesulam, M. M., & Hurley, R. S. (2017). Functional Connectivity is Reduced in Early-stage Primary Progressive Aphasia When Atrophy is not Prominent. *Alzheimer Disease and Associated Disorders*, *31*(2), 101–106. https://doi.org/10.1097/WAD.0000000000000193

Borghesani, V., Hinkley, L.B., Ranasinghe, K., Thompson, M., Shwe, W., Mizuiri, D., Honma, S., Henry, M., Houde, J.F., Miller, Z., Nagarajan, S.S., & Gorno-Tempini, M.L. (2020) Taking the sub-lexical route: the spatiotemporal dynamics of reading in semantic variant of Primary Progressive Aphasia.

695 Brain

696 Borghesani, V., Pedregosa, F., Buiatti, M., Amadon, A., Eger, E., & Piazza, M. (2016). Word meaning in
697 the ventral visual path: a perceptual to conceptual gradient of semantic coding. *NeuroImage*, *143*,
698 128–140. https://doi.org/10.1016/j.neuroimage.2016.08.068

699 Borghesani, V., & Piazza, M. (2017). The neuro-cognitive representations of symbols: the case of
700 concrete words. *Neuropsychologia*, *105*(June), 4–17.
701 https://doi.org/10.1016/j.neuropsychologia.2017.06.026

702 Bruffaerts, R., Tyler, L. K., Shafto, M., Tsvetanov, K. A., Centre, C., & Clarke, A. (2019). Perceptual and
703 conceptual processing of visual objects across the adult lifespan, (February), 1–13.
704 https://doi.org/10.1038/s41598-019-50254-5

705 Caramazza, A., & Shelton, J. R. (1998). Domain-Specific Knowledge Systems in the Brain: The Animate-
706 Inanimate Distinction. *Journal of Cognitive Neuroscience*, *10*(1), 1–34.
707 https://doi.org/10.1162/089892998563752

708 Chiou, R., Humphreys, G. F., Jung, J. Y., & Lambon Ralph, M. A. (2018). *Controlled semantic cognition*
709 *relies upon dynamic and flexible interactions between the executive 'semantic control' and hub-*
710 *and-spoke 'semantic representation' systems*. *Cortex* (Vol. 103). Elsevier Ltd.
711 https://doi.org/10.1016/j.cortex.2018.02.018

712 Clarke, A., & Tyler, L. K. (2015). Understanding What We See: How We Derive Meaning From Vision.
713 Trends in Cognitive Sciences, 19(11), 677–687. https://doi.org/10.1016/j.tics.2015.08.008

714 Clarke, A., Taylor, K. I., & Tyler, L. K. (2011). The evolution of meaning: spatio-temporal dynamics of
715 visual object recognition. *Journal of Cognitive Neuroscience*, *23*(8), 1887–1899.
716 https://doi.org/10.1162/jocn.2010.21544

717 Collins, J. A., Montal, V., Hochberg, D., Quimby, M., Mandelli, M. L., Makris, N., … Dickerson, B. C. (2016).
718 Focal temporal pole atrophy and network degeneration in semantic variant primary progressive
719 aphasia. *Neurology*, *86*(16), 1–15. https://doi.org/10.1093/brain/aww313

720 Coutanche, M. N., & Thompson-Schill, S. L. (2015). Creating concepts from converging features in human
721 cortex. *Cerebral Cortex*, *25*(9), 2584–2593. https://doi.org/10.1093/cercor/bhu057

722 Dalal, S. S., Guggisberg, A. G., Edwards, E., Sekihara, K., Findlay, A. M., Canolty, R. T., … Nagarajan, S. S.
723 (2008). Five-dimensional neuroimaging: Localization of the time-frequency dynamics of cortical
724 activity. *NeuroImage*, *40*(4), 1686–1700. https://doi.org/10.1016/j.neuroimage.2008.01.023

725 Diehl, J., Grimmer, T., Drzezga, A., Riemenschneider, M., Förstl, H., & Kurz, A. (2004). Cerebral metabolic
726 patterns at early stages of frontotemporal dementia and semantic dementia. A PET study.
727 *Neurobiology of Aging*, *25*(8), 1051–1056. https://doi.org/10.1016/j.neurobiolaging.2003.10.007

728 Donner, T. H., & Siegel, M. (2011). A framework for local cortical oscillation patterns. Trends in cognitive

sciences, 15(5), 191-199.

Downing, P. E., Wiggett, A. J., & Peelen, M. V. (2007). Functional Magnetic Resonance Imaging Investigation of Overlapping Lateral Occipitotemporal Activations Using Multi-Voxel Pattern Analysis. *Journal of Neuroscience*, *27*(1), 226–233. https://doi.org/10.1523/JNEUROSCI.3619-06.2007

Downing, P., & Kanwisher, N. (2001). A cortical area specialized for visual processing of the human body. *Journal of Vision*, *1*(3). https://doi.org/10.1167/1.3.341

Epstein, R., & Kanwisher, N. (1998). The parahippocampal place area: A cortical representation of the local visual environment. *NeuroImage*, *7*(4 PART II), 6–9. https://doi.org/10.1016/s1053-8119(18)31174-1

Fernandino L, Binder JR, Desai RH, Pendl SL, Humphries CJ, Gross WL, Conant LL, Seidenberg MS (2015b) Concept Representation Reflects Multimodal Abstraction: A Framework for Embodied Semantics. Cereb Cortex 26:2018–2034.

Folstein, M. F., Folstein, S. E., & McHugh, P. R. (1975). "Mini-mental state": A practical method for grading the cognitive state of patients for the clinician. *Journal of Psychiatric Research, 12*(3), 189–198.

Galantucci, S., Tartaglia, M. C., Wilson, S. M., Henry, M. L., Filippi, M., Agosta, F., … Gorno-Tempini, M. L. (2011). White matter damage in primary progressive aphasias: A diffusion tensor tractography study. *Brain*, *134*(10), 3011–3029. https://doi.org/10.1093/brain/awr099

Gauthier, I., Tarr, M. J., Moylan, J., Skudlarski, P., Gore, J. C., & Anderson, A. W. (2000). The fusiform "face area" is part of a network that processes faces at the individual level. *Journal of Cognitive Neuroscience*, *12*(3), 495–504. https://doi.org/10.1162/089892900562165

Gorno-Tempini M, Dronkers N, Rankin K, Ogar J, Phengrasamy L, Rosen H, et al. Cognition and anatomy in three variants of primary progressive aphasia. Ann Neurol 2004; 55: 335–46.

Gorno-tempini, M. L., Hillis, A. E., Weintraub, S., Kertesz, A., Mendez, M., Cappa, S., … Grossman, M. (2011). Classification of primary progressive aphasia and its variants. *Neurology*, *02*, 1–10.

Grill-Spector, K., & Weiner, K. S. (2014). The functional architecture of the ventral temporal cortex and its role in categorization. *Nature Reviews Neuroscience*, *15*(8), 536–548. https://doi.org/10.1038/nrn3747

Guo, C. C., Gorno-Tempini, M. L., Gesierich, B., Henry, M., Trujillo, A., Shany-Ur, T., … Seeley, W. W. (2013). Anterior temporal lobe degeneration produces widespread network-driven dysfunction. Brain, 136(10), 2979–2991. https://doi.org/10.1093/brain/awt222

Gwilliams, L., & King, J.-R. (2019). Recurrent Processes Emulate a Cascade of Hierarchical Decisions: Evidence from Spatio-Temporal Decoding of Human Brain Activity. *BioRxiv*, 840074.

https://doi.org/10.1101/840074

Hagoort P, Hald L, Bastiaansen M, Petersson KM (2004) Integration of word meaning and world knowledge in language comprehension. Science 304:438-441.

Hodges JR, Patterson K, Oxbury S, Funnell E. Semantic dementia.Progressive fluent aphasia with temporal lobe atrophy. Brain 1992; 115: 1783–806.

Hodges, J. R., & Patterson, K. (2007). Semantic dementia: a unique clinicopathological syndrome. *Lancet Neurology*, *6*(11), 1004–1014. https://doi.org/10.1016/S1474-4422(07)70266-1

Hoffman, P., Evans, G. A. L., & Lambon Ralph, M. A. (2014). The anterior temporal lobes are critically involved in acquiring new conceptual knowledge: Evidence for impaired feature integration in semantic dementia. *Cortex*, *50*(1), 19–31. https://doi.org/10.1016/j.cortex.2013.10.006

Hoffman, P., Jones, R. W., & Ralph, M. A. L. (2012). The degraded concept representation system in semantic dementia: Damage to pan-modal hub, then visual spoke. *Brain*, *135*(12), 3770–3780. https://doi.org/10.1093/brain/aws282

Huth, A. G., Nishimoto, S., Vu, A. T., & Gallant, J. L. (2012). A Continuous Semantic Space Describes the Representation of Thousands of Object and Action Categories across the Human Brain. *Neuron*, *76*(6), 1210–1224. https://doi.org/10.1016/j.neuron.2012.10.014

Jefferies, E., & Lambon Ralph, M. A. (2006). Semantic impairment in stroke aphasia versus semantic dementia: A case-series comparison. *Brain*, *129*(8), 2132–2147. https://doi.org/10.1093/brain/awl153

Kanwisher, N., McDermott, J., & Chun, M. M. (1997). The fusiform face area: a module in human extrastriate cortex specialized for face perception. *The Journal of Neuroscience : The Official Journal of the Society for Neuroscience*, *17*(11), 4302–4311. https://doi.org/10.1098/Rstb.2006.1934

Kielar, A., Deschamps, T., Jokel, R., & Meltzer, J. A. (2018). Abnormal language-related oscillatory responses in primary progressive aphasia. *NeuroImage: Clinical*, *18*(2017), 560–574. https://doi.org/10.1016/j.nicl.2018.02.028

Kielar A, Panamsky L, Links KA, Meltzer JA (2015) Localization of electrophysiological responses to semantic and syntactic anomalies in language comprehension with MEG. Neuroimage 105:507-524.

Kietzmann, T. C., Spoerer, C. J., Sörensen, L. K. A., Cichy, R. M., & Hauk, O. (2019). Recurrence is required to capture the representational dynamics of the human visual system. https://doi.org/10.1073/pnas.1905544116

Koenig, P., Smith, E. E., & Grossman, M. (2006). Semantic categorisation of novel objects in frontotemporal dementia. *Cognitive Neuropsychology*, *23*(4), 541–562.

https://doi.org/10.1080/02643290542000094

Lacombe, J., Jolicoeur, P., Grimault, S., Pineault, J., & Joubert, S. (2015). Neural changes associated with semantic processing in healthy aging despite intact behavioral performance. *Brain and Language*, *149*, 118–127. https://doi.org/10.1016/j.bandl.2015.07.003

Laiacona, M., & Capitani, E. (2001). A Case of Prevailing Deficit of Nonliving Categories or a Case of Prevailing Sparing of Living Categories? *Cognitive Neuropsychology*, *18*(1), 39–70. https://doi.org/10.1080/02643290042000035

Laiacona, M., Capitani, E., & Caramazza, A. (2003). Category-specific Semantic Deficits do not Reflect the Sensory/Functional Organization of the Brain: A Test of the "Sensory Quality" Hypothesis. *Neurocase*, *9*(3), 221–231. https://doi.org/10.1076/neur.9.3.221.15562

Lambon-Ralph, M. A., Jefferies, E., Patterson, K., & Rogers, T. T. (2016). The neural and computational bases of semantic cognition. *Nature Reviews Neuroscience*, *18*(1), 42–55. https://doi.org/10.1038/nrn.2016.150

Lambon-Ralph, M. A., Jefferies, E., Patterson, K., & Rogers, T. T. (2017). The neural and computational bases of semantic cognition. *Nature Reviews Neuroscience*, *18*(1), 42–55. https://doi.org/10.1038/nrn.2016.150

Lambon-Ralph, M. A., Sage, K., Jones, R. W., & Mayberry, E. J. (2010). Coherent concepts are computed in the anterior temporal lobes. *Proceedings of the National Academy of Sciences*, *107*(6), 2717–2722. https://doi.org/10.1073/pnas.0907307107

Lambon Ralph, M. A., Lowe, C., & Rogers, T. T. (2007). Neural basis of category-specific semantic deficits for living things: Evidence from semantic dementia, HSVE and a neural network model. *Brain*, *130*(4), 1127–1137. https://doi.org/10.1093/brain/awm025

Lerner, Y., Hendler, T., Ben-Bashat, D., Harel, M., & Malach, R. (2001). A Hierarchical Axis of Object Processing Stages in the Human Visual Cortex. *Cerebral Cortex*, *11*(4), 287–297. https://doi.org/10.1093/cercor/11.4.287

Makeig, S., Debener, S., Onton, J., & Delorme, A. (2004). Mining event-related brain dynamics. Trends in cognitive sciences, 8(5), 204-210.

Maguire, E. A., Kumaran, D., Hassabis, D., & Kopelman, M. D. (2010). Autobiographical memory in semantic dementia: A longitudinal fMRI study. *Neuropsychologia*, *48*(1), 123–136. https://doi.org/10.1016/j.neuropsychologia.2009.08.020

Mandelli, M. L., Caverzasi, E., Binney, R. J., Henry, M. L., Lobach, I., Block, N., … Gorno-Tempini, M. L. (2014). Frontal white matter tracts sustaining speech production in primary progressive aphasia. *Journal of Neuroscience*, *34*(29), 9754–9767. https://doi.org/10.1523/JNEUROSCI.3464-13.2014

Martin, A., & Chao, L. (2001). Semantic memory and the brain: structure and processes. *Current*

Opinions in Neurobiology, *11*, 194–201.

Montembeault, M., Chapleau, M., Jarret, J., Boukadi, M., Laforce, R., Wilson, M. A., … Brambati, S. M. (2019). Differential language network functional connectivity alterations in Alzheimer's disease and the semantic variant of primary progressive aphasia. *Cortex*, *117*, 284–298. https://doi.org/10.1016/j.cortex.2019.03.018

Moss, H. E., Rodd, J. M., Stamatakis, E. A., Bright, P., & Tyler, L. K. (2005). Anteromedial temporal cortex supports fine-grained differentiation among objects. *Cerebral Cortex*, *15*(5), 616–627. https://doi.org/10.1093/cercor/bhh163

Mummery, C. J., Patterson, K., Wise, R. J. S., Vandenbergh, R., Price, C. J., & Hodges, J. R. (1999). Disrupted temporal lobe connections in semantic dementia. *Brain*, *122*(1), 61–73. https://doi.org/10.1093/brain/122.1.61

Peelen, M. V, & Caramazza, A. (2012). Conceptual object representations in human anterior temporal cortex. *The Journal of Neuroscience*, *32*(45), 15728–15736. https://doi.org/10.1523/JNEUROSCI.1953-12.2012

Pietrini, V., Nertempi, P., Vaglia, A., Revello, M. G., Pinna, V., & Ferro-Milone, F. (1988). Recovery from herpes simplex encephalitis: Selective impairment of specific semantic categories with neuroradiological correlation. *Journal of Neurology, Neurosurgery & Psychiatry*, *51*, 1284–1293. https://doi.org/10.1136/jnnp.51.10.1284

Pineault, J., Jolicœur, P., Grimault, S., Lacombe, J., Brambati, S. M., Bier, N., … Meg, A. (2019). A MEG study of the neural substrates of semantic processing in semantic variant primary progressive aphasia. *Neurocase*, *25*(3–4), 118–129. https://doi.org/10.1080/13554794.2019.1631853

Price, C. J., Crinion, J., & Friston, K. J. (2006). Design and Analysis of fMRI Studies With Neurologically Impaired Patients, *826*, 816–826. https://doi.org/10.1002/jmri.20580

Price, C. J., & Friston, K. J. (2002). Degeneracy and cognitive anatomy. *Trends in Cognitive Sciences*, *6*(10), 416–421.

Ranasinghe, K. G., Hinkley, L. B., Beagle, A. J., Mizuiri, D., Honma, S. M., Welch, A. E., … Nagarajan, S. S. (2017). Distinct spatiotemporal patterns of neuronal functional connectivity in primary progressive aphasia variants. *Brain*, *140*(10), 2737–2751. https://doi.org/10.1093/brain/awx217

Robinson, S., & Vrba, J. (1999). Functional neuroimaging by synthetic aperture magnetometry (SAM). In Yoshimoto (Ed.), *Recent advances in biomagnetism* (pp. 302–305). Sendai, Japan: Tohoku University.

Sacchett, C., & Humphreys, G. W. (1992). Calling a squirrel a squirrel but a canoe a wigwam: a category-specific deficit for artefactual objects and body parts. *Cognitive Neuropsychology*, *9*(1), 73–86. https://doi.org/10.1080/02643299208252053

Sami, S., Williams, N., Hughes, L. E., Cope, T. E., Rittman, T., Coyle-Gilchrist, I. T. S., … Rowe, J. B. (2018). Neurophysiological signatures of Alzheimer's disease and frontotemporal lobar degeneration: Pathology versus phenotype. *Brain*, *141*(8), 2500–2510. https://doi.org/10.1093/brain/awy180

Sartori, G., Job, R., Miozzo, M., Zago, S., & Marchiori, G. (1993). Category-specific form-knowledge deficit in a patient with herpes simplex virus encephalitis. *Journal of Clinical and Experimental Neuropsychology*, *15*(August 2015), 280–299. https://doi.org/10.1080/01688639308402563

Singh, K. D., Barnes, G. R., & Hillebrand, A. (2003). Group imaging of task-related changes in cortical synchronisation using nonparametric permutation testing. *NeuroImage*, *19*(4), 1589–1601. https://doi.org/10.1016/S1053-8119(03)00249-0

Thorat, S., Proklova, D., & Peelen, M. V. (2019). The nature of the animacy organization in human ventral temporal cortex, 1–18. Retrieved from http://arxiv.org/abs/1904.02866

van Ackeren MJ, Schneider TR, Musch K, Rueschemeyer SA (2014) Oscillatory neuronal activity reflects lexical-semantic feature integration within and across sensory modalities in distributed cortical networks. The Journal of neuroscience : the official journal of the Society for Neuroscience 34:14318-14323

Viard, A., Desgranges, B., Matuszewski, V., Lebreton, K., Belliard, S., De La Sayette, V., … Piolino, P. (2013). Autobiographical memory in semantic dementia: New insights from two patients using fMRI. *Neuropsychologia*, *51*(13), 2620–2632. https://doi.org/10.1016/j.neuropsychologia.2013.08.007

Viard, A., Piolino, P., Belliard, S., De La Sayette, V., Desgranges, B., & Eustache, F. (2014). Episodic future thinking in semantic dementia: A cognitive and fMRI Study. *PLoS ONE*, *9*(10). https://doi.org/10.1371/journal.pone.0111046

Warrington, E. K., & Shallice, T. (1984). Category Specific Semantic Impairments. *Brain*, *107*(3), 829–853. https://doi.org/10.1093/brain/107.3.829

Wilson, S. M., Brambati, S. M., Henry, R. G., Handwerker, D. A., Agosta, F., Miller, B. L., … Gorno-Tempini, M. L. (2009). The neural basis of surface dyslexia in semantic dementia. *Brain*, *132*(1), 71–86. https://doi.org/10.1093/brain/awn300

Wilson, S., Yen, M., & Eriksson, D. (2018). An adaptive semantic matching paradigm for reliable and valid language mapping in individuals with aphasia, (February). https://doi.org/10.1002/hbm.24077